

Equatorial electrodynamics and neutral background in the Asian sector during the 2009 stratospheric sudden warming

Huixin Liu,^{1,2} Mamoru Yamamoto,³ S. Tulasi Ram,³ Takuya Tsugawa,⁴ Yuichi Otsuka,⁵ Claudia Stolle,⁶ Eelco Doornbos,⁷ Kiyohumi Yumoto,^{1,2} and Tsutomu Nagatsuma⁴

Received 28 February 2011; revised 9 May 2011; accepted 19 May 2011; published 17 August 2011.

[1] Using ground observations of total electron content (TEC) and equatorial electrojet (EEJ) in the Asian sector, along with plasma and neutral densities obtained from the CHAMP satellite, we investigate the ionospheric electrodynamics and neutral background in this longitude sector during the major stratospheric sudden warming (SSW) in January 2009. Our analysis reveals the following prominent features. First, the TEC response in tropical regions is strongly latitude dependent, with monotonic depletion at the dip equator but a semidiurnal perturbation at low latitudes. Second, the TEC semidiurnal perturbation possesses a significant hemispheric asymmetry in terms of onset date and magnitude. It starts on the same day as the SSW peak in the Northern Hemisphere but 2 days later in the Southern Hemisphere. Its magnitude is twice as strong in the north than in the south. Third, strong counter electrojet occurs in the afternoon, following the strengthening of the eastward EEJ in the morning. Fourth, semidiurnal perturbation in both TEC and EEJ possesses a phase shift, at a rate of about 0.7 h/day. Comparisons with results reported in the Peruvian sector reveal clear longitude dependence in the amplitude and hemispheric asymmetry of the semidiurnal perturbation. Finally, thermospheric density undergoes ~25% decrease at low latitudes in the afternoon local time sector during the SSW, indicating significant cooling effects in the tropical upper thermosphere.

Citation: Liu, H., M. Yamamoto, S. Tulasi Ram, T. Tsugawa, Y. Otsuka, C. Stolle, E. Doornbos, K. Yumoto, and T. Nagatsuma (2011), Equatorial electrodynamics and neutral background in the Asian sector during the 2009 stratospheric sudden warming, *J. Geophys. Res.*, 116, A08308, doi:10.1029/2011JA016607.

1. Introduction

[2] The Earth's ionosphere is the ionized part of the upper atmosphere, occupying the space between about 90 to 1000 km altitude. It reacts to energy and momentum input from various forcing agents, like the EUV/UV radiation from the Sun, particle precipitation and Joule heating controlled by the magnetosphere, neutral wind and composition in the background thermosphere, and tides and waves from the lower atmosphere. In general, the solar and magnetospheric forcing is dominating. Their effects on the ionosphere are

dramatic, hence easy to detect and comprehensively documented [e.g., Prölss, 1980, 1993; Liu *et al.*, 2007a, and references therein]. On the other hand, forcing from the lower atmosphere is normally much weaker, and their effects are subtle and difficult to detect. However, owing to improved resolution and accuracy of recent ground and spaceborne instruments, together with the passing of the deep solar minimum in solar cycle 23, various ionospheric features driven by the lower atmosphere forcing have been rapidly identified. A few important examples are the quasi 2 day, 16 day wave signatures [Forbes and Leveroni, 1992; Pancheva *et al.*, 2006; Abdu *et al.*, 2006; Lastovicka, 2006], the wave 4 longitudinal structure driven mainly by the tropical deep convection [Sagawa *et al.*, 2005; Immel *et al.*, 2006; Wan *et al.*, 2008; Liu *et al.*, 2009], and the semidiurnal perturbation driven by sudden stratospheric warming (SSW) events [e.g., Goncharenko and Zhang, 2008; Chau *et al.*, 2009; Goncharenko *et al.*, 2010a, 2010b; Fejer *et al.*, 2010]. They demonstrate the close linkage between the ionosphere and lower atmosphere in both time and spatial domains.

[3] Among the examples just given, the ionosphere–lower atmosphere coupling during SSWs is unique in that it involves processes at all latitudes from the equator to the pole. Phenomenon-wise, sudden stratosphere warming is a meteorological event where the stratospheric temperature experiences a rapid and significant rise of more than a few

¹Department of Earth and Planetary Science, Kyushu University, Fukuoka, Japan.

²Space Environment Research Center, Kyushu University, Fukuoka, Japan.

³Research Institute for Sustainable Humanosphere, Kyoto University, Kyoto, Japan.

⁴National Institute of Information and Communications Technology, Koganei, Japan.

⁵Solar–Terrestrial Environment Laboratory, Nagoya University, Nagoya, Japan.

⁶National Space Institute, DTU Space, Technical University of Denmark, Copenhagen, Denmark.

⁷Aerospace Engineering, Delft University of Technology, Delft, Netherlands.

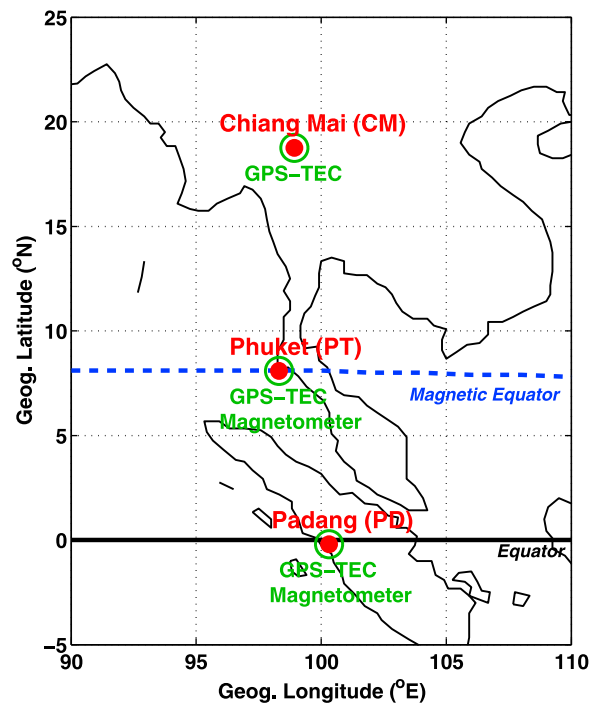


Figure 1. A map of Southeast Asia, showing locations of the ground stations used in this study.

tens Kelvin in the winter polar region. It was first discovered by Scherhag [1952]. The well accepted generation mechanism was proposed by Matsuno [1971], which involves mainly planetary wave–mean wind interaction in the polar region and global-scale meridional circulation. The SSW effect does not confine itself only in the polar stratosphere, but extends in altitudes and latitudes. In the polar region, mesosphere cooling and lower thermosphere warming have been predicted and observationally confirmed [see, e.g., Liu and Roble, 2002; Funke et al., 2010; Kurihara et al., 2010]. At middle latitudes, radar observations reveal alternating cooling and warming regions in the ionosphere E and F region [Goncharenko and Zhang, 2008]. At low and equatorial latitudes, significant cooling accompanying SSWs has long been reported in the stratosphere [Julian and Labitzke, 1965; Fritz and Soules, 1970, 1972]. More than 100 km up in the ionosphere, a semidiurnal perturbation has been identified during SSW events in various parameters like the vertical plasma drift, equatorial electrojet (EEJ), and the total electron content (TEC) [Chau et al., 2009, 2010; Vineeth et al., 2009; Sridharan et al., 2009; Fejer et al., 2010; Goncharenko et al., 2010a, 2010b].

[4] Since the temperature and polar vortex in the polar stratosphere during SSWs have distinct longitudinal structures, it is natural to speculate a longitude dependence in its effects on other atmospheric regions. Such longitude dependence in the ionosphere has been recently shown by Liu et al. [2010] using model simulations, and is explained to be mainly caused by the amplitudes and phases of the superposing wave components. Their results show that the semidiurnal perturbation tend to maximize in the Peruvian sector. In this study, we present observations in the Asian sector during the well-reported 2009 major warming event and compare them with reported results in the Peruvian sector.

Our observations include TEC and EEJ measurements from ground instruments, and plasma and neutral density from the CHAMP satellite. With this, we wish to examine not only the electrodynamics of the ionosphere, but also the neutral background during the SSW period.

2. Data

[5] Both ground and satellite observations are employed in this study. Most ground data come from the SEALION network. SEALION stands for South East Asia Low-latitude Ionospheric Network, focusing on monitoring and forecasting equatorial ionospheric disturbances [Maruyama et al., 2007]. It is unique in having conjugate observational points in the Northern and Southern hemispheres and around the magnetic dip equator. Measurements of absolute TEC from two SEALION stations at Chiang Mai (18.8°N, 98.9°E geographic) and Phuket (8.1°N, 98.3°E geographic), along with another station at Padang (0.2°S, 100.1°E geographic) are used in this study. Locating at dip latitudes of 12.7°N, 0.2°S, and 10.1°S, respectively, a combination of these three stations provides a measure of the structure and dynamics of the equatorial ionization anomaly along 99°E longitude. The method for obtaining absolute TEC is given by Otsuka et al. [2002]. The EEJ intensity at Phuket during the 2009 SSW event is also obtained from the difference between the horizontal component of the magnetic field at Phuket and at Padang, which is a classical method given by Rusch and Richmond [1973]. The relative locations of these stations are displayed on the map in Figure 1.

[6] Plasma and neutral density observations from the CHAMP satellite are also employed. CHAMP was in a near-circular orbit with an inclination of 87.3° and an initial height of ~450 km at launch in July 2000. The mission ended on 19 September 2010, after 10 years of successful flight. The satellite probed the in situ thermospheric density with a triaxial accelerometer and the in situ electron density with a Planar Langmuir probe. Its orbit was near 325 km altitude during January 2009, hence all measurements are normalized to this fixed altitude to remove density variations due to height changes of satellite orbits. Readers are referred to Liu et al. [2005, 2006, 2007b] and McNamara et al. [2007] for details concerning the derivation and processing procedure.

3. Results

3.1. TEC Observations

[7] Figure 2 displays the TEC variation as a function of local time (LT) and day of year (DOY) in 2009 at Chiang Mai (CM), Phuket (PT) and Padang (PD). The 3 h Kp index during the same period is shown in the fourth panel of Figure 2, indicating an overall quiet geomagnetic condition with occasional minor disturbances. The development of the SSW is indicated by the solid lines in the first, second, and third panels, which is the average stratospheric temperature at 10 hPa for latitudes above 70°N in the northern polar region obtained from the National Center for Environmental Predictions (NCEP) reanalysis. The peak warming occurred on 23 January 2009, and the major warming criteria is met on 24 January, when the zonal wind (not shown) at 60°N turned from eastward to westward.

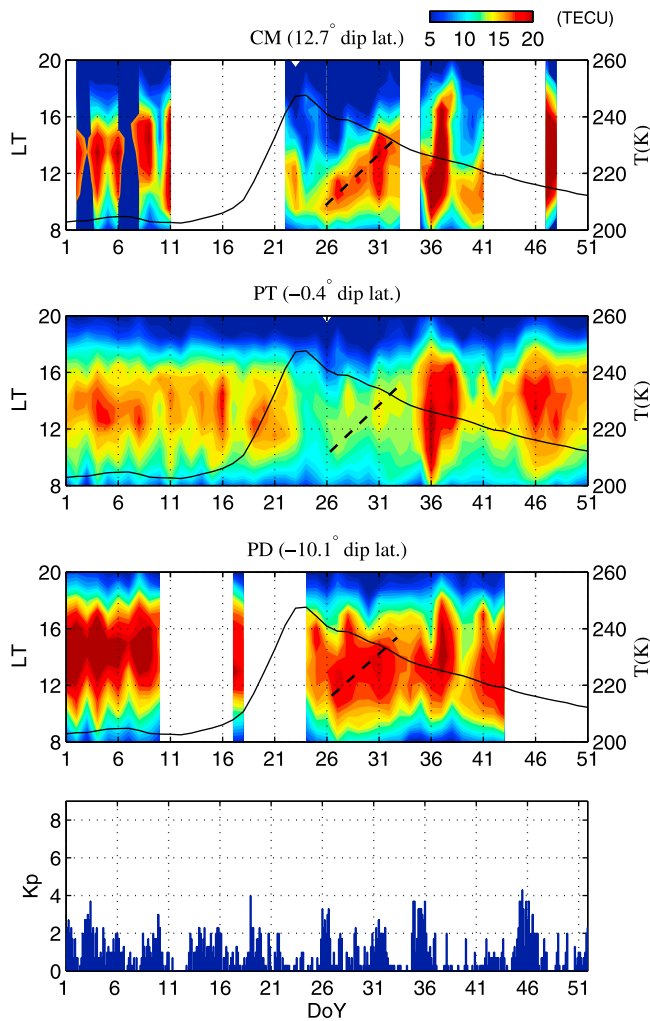


Figure 2. TEC variation with LT and day of year (DOY) in 2009 at three ground stations at Chiang Mai (CM), Phuket (PT), and Padang (PD). The three stations are all near 99° E geographic longitude. Solid curves represent stratospheric temperature at 10 hPa averaged between 70° N and 90° N from the NCEP reanalysis. The fourth panel shows the 3 h K_p index.

[8] In spite of some data gaps, several prominent features are noted. In early January before the SSW peak, the TEC exhibits a normal diurnal variation, with a maximum around 14:00 LT. The magnitude of the diurnal variation shows a clear 2 day oscillation at all three stations, which may be a sign for the 2 day wave [Pancheva *et al.*, 2006]. This diurnal pattern is disrupted along with the occurrence of the SSW. This is seen as an overall depletion around the SSW peak on 23–24 January, followed by unusual daily variations until about 31 January. During this period, the maximum TEC first appears in the early morning, e.g., 09:00 LT on 25 January at CM, then shifts consistently to later local time with the progress of days. This results in a prominent tilted structure. The TEC experiences strong enhancement around $\text{DOY} = 35\text{--}38$, likely as a consequence of the increased and lasting geomagnetic activity during this period. These gross features of the TEC are similar to those observed in the Peruvian sector [Goncharenko *et al.*, 2010b, 2010a]. In the

following, we look into important details about the structure and dynamics and discuss its similarity and difference from that in the Peruvian sector. The 2 day wave seen before the SSW and its possible response to the SSW are interesting phenomena on their own, which we investigate in a separate study.

[9] First, we examine the unusual diurnal variation during 23–31 January 2009. Figure 3 presents the TEC in line plots for the period during 23–31 January for all three stations. The dashed lines represent quiet time references, which are obtained by averaging TECs during 2–11 January 2009 at each corresponding station. This period is characterized with very low K_p levels, and has also been used as quiet reference by Goncharenko *et al.* [2010a] in their study on the Peruvian sector during the same event. Taking the same period thus facilitates comparisons between these sectors.

[10] Main features pertain to the TEC variation during the SSW are described as follows: (1) at the dip equator (PT) as seen in Figure 3 (middle), an overall drop of the TEC value throughout the daytime occurs during the whole period of 23–31 January, with maximum depletion around 26–27 January; (2) in the Equatorial Ionization Anomaly (EIA) crest regions (CM and PD), TEC exhibits a semidiurnal perturbation, with morning enhancement and afternoon depletion in comparison to the quiet time TEC; (3) this semidiurnal pattern shows a continuous phase shift to later local time, with an average shifting rate of about 0.7 h/day as indicated by the dashed lines; and (4) the onset of the semidiurnal perturbation is on 23 January in the Northern Hemisphere, and on 25 January in the Southern Hemisphere.

[11] Figure 4 examines the magnitude of the perturbation (difference between the solid and dashed lines in Figure 3) in terms of percentage. The morning enhancements around 09:00 LT are shown as solid lines, while the afternoon depletion around 15:00 LT as dash-dotted ones. It is seen that the morning enhancement is of comparable magnitude at CM and PD. The afternoon depletion, however, shows a strong hemispheric asymmetry. The depletion is at a rather constant level around -15% in the Southern Hemisphere (PD) throughout 25–31 January. In the Northern Hemisphere (CM), it reaches deeper than -50% on 26/27 January, and recovers rapidly thereafter. Thus, the amplitude of the semidiurnal perturbation, as indicated by the difference between the morning enhancement and the afternoon depletion, is about double in the Northern Hemisphere as that in the Southern Hemisphere.

[12] Next, we see how the whole EIA structure behaves. Figure 5 displays the TEC variation around 09:00 and 15:00 LT at three stations. Figure 5 (left) displays TEC variation with DOY during 1–31 January, while Figure 5 (right) displays the latitude distribution before and after the SSW peak. It is seen that the TEC is nearly constant during the period between 2 and 10 January, hence further justifying the use of this period as the quiet time reference. Before the occurrence of the SSW, no clear EIA structures develop in either the morning or evening sector as indicated by the dashed lines in Figures 5c and 5d. After the SSW peak on 23 January, a strong EIA structure develops in the morning sector (solid line in Figure 5c), with more than 20% increase in both crest regions and a simultaneous $\sim 20\%$ depletion in the trough region. In the afternoon sector (solid line in Figure 5d), strong depletion occurs throughout the equatorial and low-

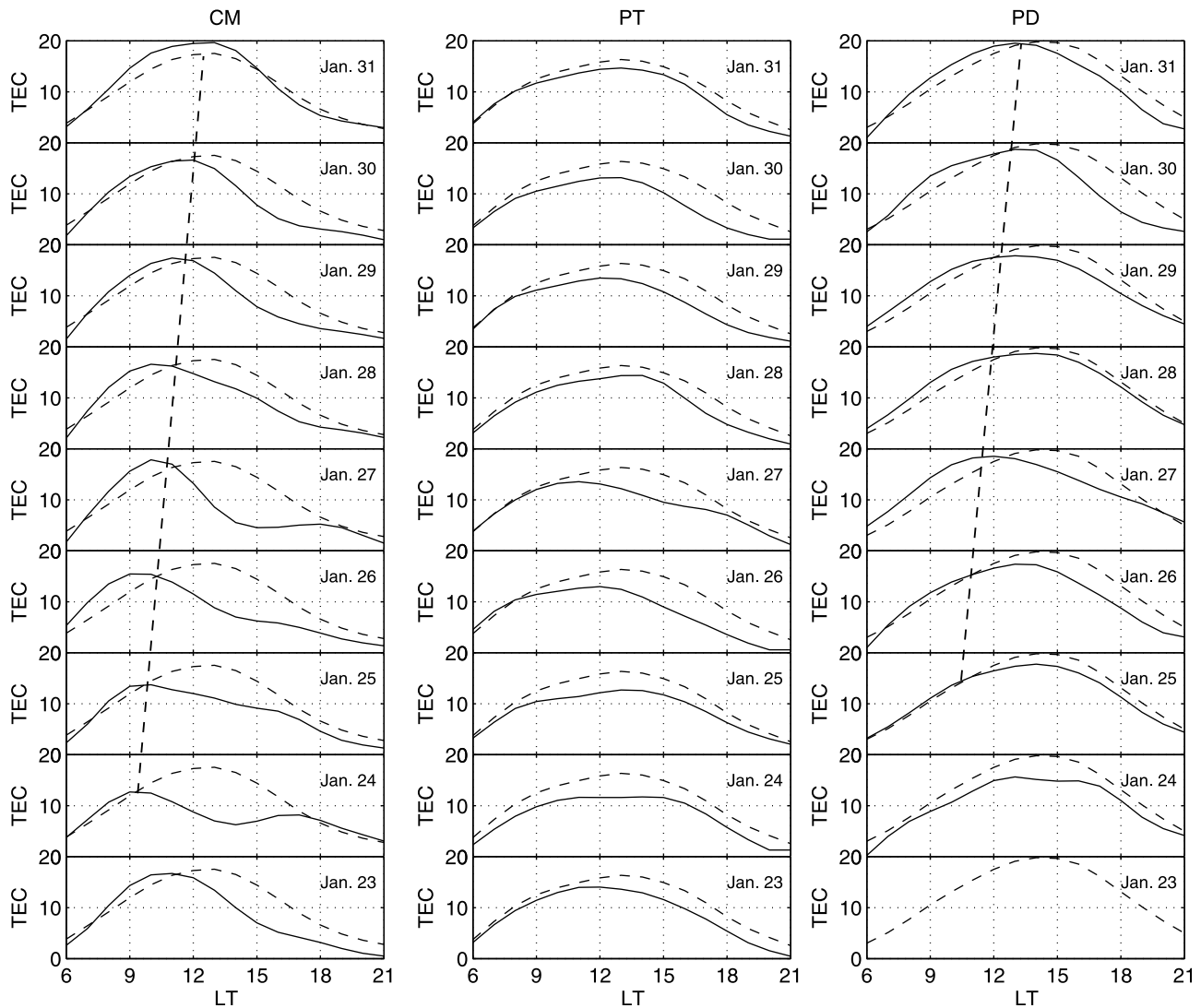


Figure 3. TEC variations during DOY 23–31 at (left) CM, (middle) PT, and (right) PD, locating in the Northern Hemisphere, on the dip equator, and in the Southern Hemisphere, respectively. Dashed curves indicate the quiet time reference values at corresponding locations.

latitude regions, but no classical EIA forms. It is further noted that the hemispheric asymmetry of the TEC reverses in the morning and afternoon sector, for periods both before and after the SSW peak. This reversal is a frequently observed feature at low solar activity levels, due to the counter acting forces from transequatorial neutral wind and the equatorial fountain [Tulasi Ram *et al.*, 2009].

3.2. Equatorial Electrojet

[13] Figure 6 displays the EEJ at Phuket as a function of LT and DOY during 1–31 January 2009. The EEJ diurnal variation remains stable before 21 January, being eastward in the noon sector and dying away after about 15:00 LT. At the same time, a 2 day oscillation is clearly evident in the magnitude of the EEJ. A strong counter electrojet (CEJ) of about -40 nT occurs in the afternoon during 23–30 January, with a brief interruption on 25 January. Accompanying these CEJs, the EEJ in the morning is significantly enhanced, with a maximum before 10:00 LT. A gradual shift of the EEJ peak to later local time is evident during 26–

30 January. Similar observations of CEJ during SSW events have been reported in the Indian sector as well [Vineeth *et al.*, 2009; Sridharan *et al.*, 2009].

[14] Taking the average EEJ diurnal variation during 2–11 January as the quiet time reference, disturbances in the morning (09:00 LT) and afternoon (15:00 LT) sectors are shown in Figure 7, expressed in percentage. It is seen that the EEJ experiences enhancement in the morning but weakening in the afternoon, hence a semidiurnal perturbation occurs during 23–31 January. The afternoon weakening is seen to be far more severe than the morning enhancement, with magnitude about -270% in comparison to 100% . These features correspond well with those of the semidiurnal perturbation in TEC shown in Figure 4. Note that no clear delay is observed between the onset of the semidiurnal perturbation and the SSW peak.

3.3. CHAMP Observations

[15] Distributions of the plasma and neutral density with latitude and DOY at 325 km altitude are presented in Figure 8 for

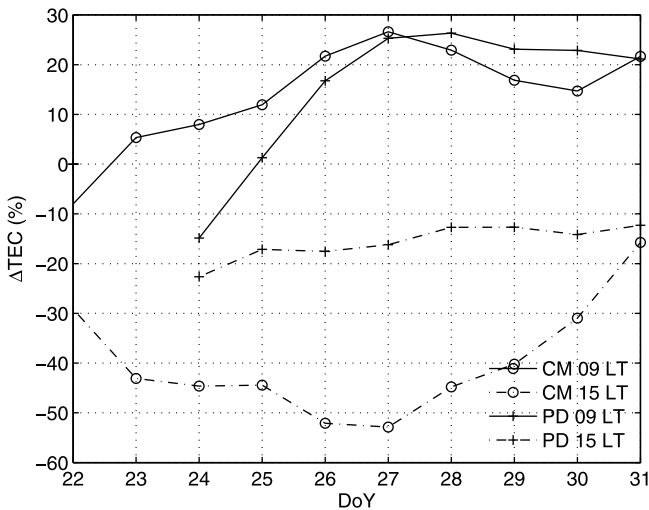


Figure 4. Variations of the TEC disturbance with DOY around 09:00 LT (averaged between 08:00 and 10:00 LT) and around 15:00 LT (averaged over 14:00–16:00 LT). The disturbance is expressed in percentage. A three-point smoothing is applied to the curves.

the SEALION longitude sector. These structures are observed between 15:30 and 17:24 LT as indicated by the solid line in Figure 8 (middle). The dip equator and stratospheric temperature at 10 hPa are indicated by the white and pink lines in Figure 8 (top), respectively. The average plasma and neutral density variations within ± 25 dip latitudes are shown in Figure 8 (bottom).

[16] The interesting feature here is the significant depletion in both the plasma and neutral density around the peak

of the SSW. It is seen that the neutral depletion occurs already on 20 January, which is before the SSW peak and the plasma depletion (see Figure 8, bottom). In the Asian sector, the depletion reaches maximum on 26 January, with a magnitude of $\sim 45\%$ for the plasma and 25% for the neutral density. When taking into account the local time change from 17:00 LT on 18 January to 16:18 LT on 26 January due to the precession of the satellite, the actual depletion would be even larger than these numbers given. This is because both the plasma and neutral density possess a diurnal variation with maximum normally around 14:00 LT, hence the density on 18 January would be higher than the values shown here if it would have been measured at the same local time of 16:18 LT as on 26 January. It is important to note that similar neutral density decrease is also observed in other longitude sectors.

4. Discussion

[17] The above analysis has revealed pronounced latitude and local time variations in the low-latitude ionospheric response to the SSW in the Asian sector. Furthermore, the CHAMP observations show that not only the plasma, but also the neutral density experiences substantial decrease during the SSW. We discuss the implications of these aspects in the following, and compare them with reported results from the Peruvian sector whenever possible.

4.1. Latitudinal Variation in Tropical Regions

[18] Remarkable differences exist between TEC response at different latitudes. At the dip equator, a monotonic depletion occurs at all local times throughout the SSW period. At low latitudes, however, a semidiurnal perturbation is observed. This clearly contrasts to TEC response in the

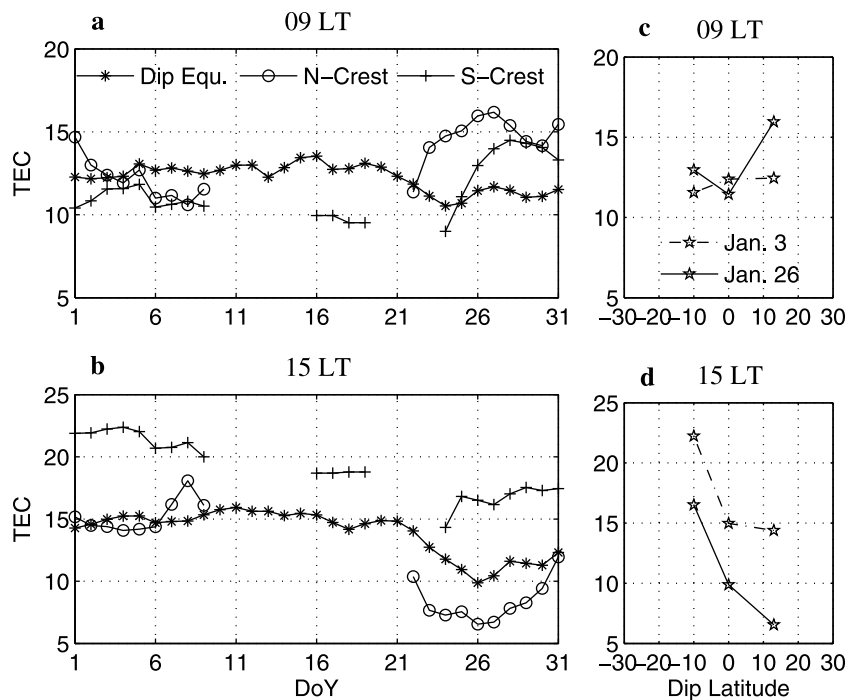


Figure 5. TEC variations (in units of TECU) at 09:00 and 15:00 LT for three stations at CM, PT, and PD. (left) The variation with DOY in January 2009. (right) Its variation with dip latitudes on 3 and 26 January.

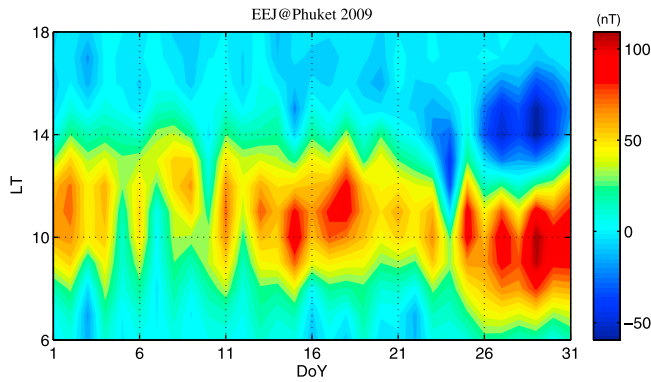


Figure 6. The equatorial electrojet observed at the equatorial station of Phuket in January 2009.

Peruvian sector, where the semidiurnal perturbation occurs also at the dip equator [see *Goncharenko et al.*, 2010b, Figure 2]. Given that enhanced upward plasma drift is observed in the Peruvian sector in the morning, depletion of the plasma density is normally expected at the dip equator. Thus, the observed enhancement in the Peruvian sector appears to be somewhat surprising and may be related to other factors like the neutral background.

[19] The semidiurnal perturbation also shows prominent differences in two sectors. First, the morning enhancement is significantly larger in the Peruvian sector than in the Asian sector, with magnitude of about 150% in comparison to 25%. This is consistent with simulation results of *Liu et al.* [2010]. Secondly, the hemispheric asymmetry in the afternoon depletion is opposite in the two sectors. Stronger depletion occurs in the Northern Hemisphere in the Asian sector (Figure 4), but in the Southern Hemisphere in the Peruvian sector [*Goncharenko et al.*, 2010a]. Hemispheric asymmetry is known to be due largely to the meridional wind in the magnetic meridian. The opposite asymmetry

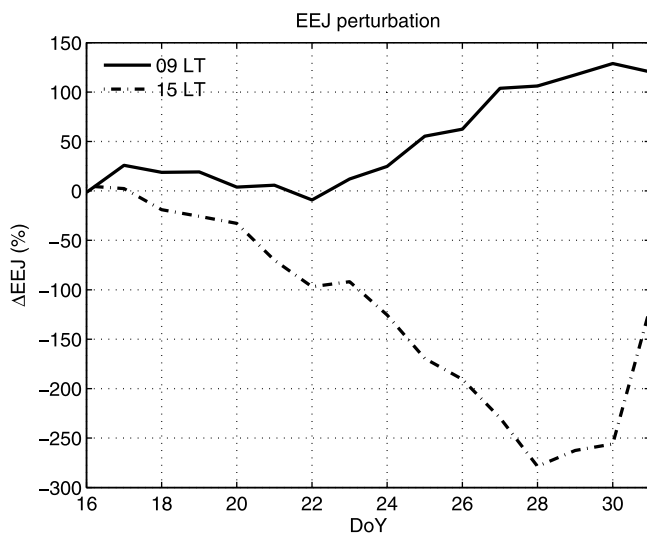


Figure 7. The EEJ disturbance around 09:00 LT (averaged between 08:00 and 10:00 LT) and around 15:00 LT (averaged over 14:00–16:00 LT) during DOY 16–31. A three-point smoothing is applied to the curves.

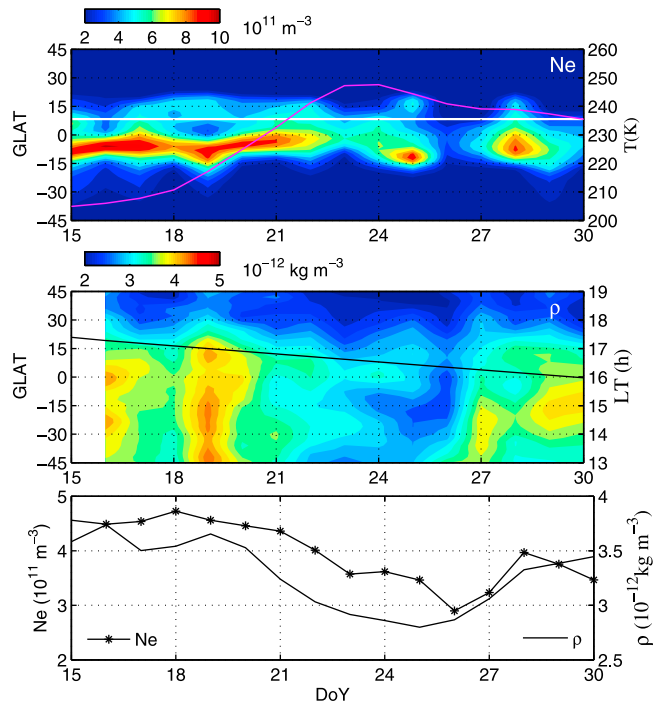


Figure 8. Distribution of the plasma and neutral density with latitude and DOY in 2009 at 325 km altitude around 99°E. (top) Pink curve is the stratosphere temperature at 10 hPa from NCEP averaged in the latitude range of 70°N–90°N; white line indicates the dip equator. (middle) Black curve indicates the local time of satellite tracks. (bottom) The plasma and neutral density averaged within ± 25 dip latitude. A three-point smoothing is applied to better show the trend.

could imply a strong longitudinal difference in the meridional wind, or different zonal wind contribution due to opposite declination angles in these two sectors. Thirdly, the onset of the semidiurnal perturbation in the Asian sector shows a 2 day delay between the Northern and Southern Hemisphere, being on 23 January 2009 in the northern crest, but on 25 January in the southern crest. This seems to indicate a southward propagation of the disturbance. However, this delay is not discernible in the Peruvian sector [*Goncharenko et al.*, 2010b, Figure 5].

[20] As to the source of the semidiurnal perturbation, *Fejer et al.* [2010] has proposed Lunar tides, whose amplitude might be enhanced during SSW. On the other hand, *Liu et al.* [2010] could reproduce the semidiurnal perturbation using the TIME-GCM model without even including the lunar tides, though they did not mention whether the perturbation exhibits a phase shift as in the observations. Thus, the source remains unclear.

[21] Although we refrain from discussing the source due to lack of sufficient evidence, we note that observations presented here allow a few comments. First, the strong contrast between the dip equator and low latitudes in the TEC response fits well with the latitudinal structure of the semidiurnal Lunar tides, with Lunar tides maximizing at low latitudes [*Pedatella and Forbes*, 2010]. Second, the phase shift rate of 0.7 h/day appears to be similar to the lunar shift of about 0.83 h/day in the moon risetime. However, the

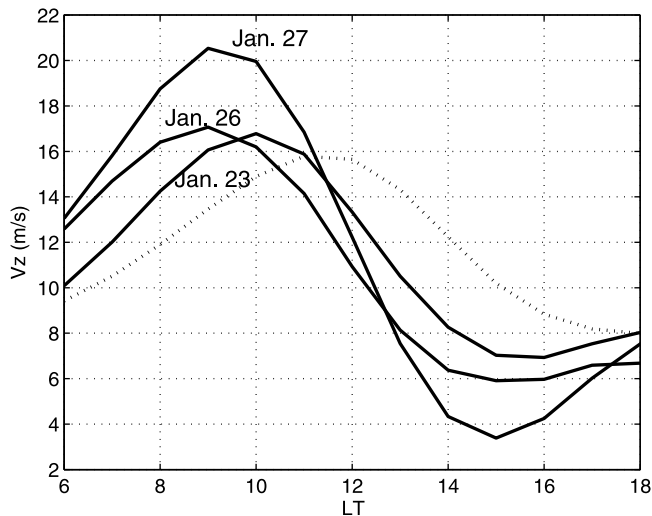


Figure 9. Vertical plasma drift inferred from the EEJ observation in the Asian sector. Positive means upward. Solid lines are for 23, 26, and 27 January. The dashed line represents the quiet time drift, obtained by averaging drifts during 2–11 January 2009.

onset of the semidiurnal perturbation on 23 January in the Northern Hemisphere seems to contradict to that reported by *Fejer et al.* [2010]. They reported a delay of the onset depending on the date of new moon. Since the nearest new moon after the SSW peak occurs on 26 January 2009, our observations thus cannot confirm such a delay.

4.2. Equatorial Electrodynamics

[22] Semidiurnal perturbations in the TEC have been claimed to be driven by a similar perturbation in the equatorial vertical plasma drift in the Peruvian sector [*Chau et al.*, 2009; *Goncharenko et al.*, 2010a, 2010b]. In the Asian sector, although measurement of the vertical plasma drift is not directly made, it can be inferred from the EEJ observations, as both the direction and amplitude of these parameters depend closely on the zonal electric field. A quantitative relation between the vertical drift and the EEJ strength is given by *Stolle et al.* [2008], as $V_z \text{ (m/s)} = 0.17 \text{ EEJ (nT)} + 7.81$ for the Peruvian sector. Due to the lack of such a reported formula for the Asian sector, we adopt this one for the Peruvian sector in our study. The obtained vertical plasma drift is shown in Figure 9 for a few example days. Quiet time drift is obtained by averaging drifts between 2 and 11 January 2009 and plotted as dashed line. It is important to note that since the formula is derived from data in the Peruvian sector, the absolute drift values shown in Figure 9 remain questionable. However, the relative variation between the quiet time and SSW time is supposed to be more reliable.

[23] It is seen that the plasma drift during SSW exhibits a clear semidiurnal perturbation, in comparison to quiet time values. But its magnitude is much smaller than in the Peruvian sector, being around 4–8 m/s (~30%) in comparison to 20 m/s (>100%). This longitudinal variation agrees well with the simulation results of *Liu et al.* [2010], showing largest drift perturbation in the Peruvian sector.

[24] As larger upward plasma drift drives stronger fountain, enhanced vertical plasma drift in the morning sector is expected to strengthen the equatorial fountain. This would consequently speed up the transport of the plasma from the dip equator to low latitudes, hence causing depletion of the plasma at the dip equator and simultaneous enhancement of the plasma at low latitudes, leading to more prominent EIA structure. This is consistent with the TEC observations shown in Figure 5c.

[25] In contrast, weakened upward plasma drift in the afternoon sector is expected to produce a plasma decrease at low latitudes but increase at the dip equator. This expectation agrees with the TEC variation at low latitudes, but disagrees with the large TEC depletion observed at the dip equator (Figure 5d). On the other hand, TEC depletion at the dip equator could be caused by a downward plasma drift, and/or changes in the background thermosphere. In case of the former, the observed TEC depletion could imply that the slope (0.17) used in the above formula is too small, and/or the offset (7.81) is too large for the Asian sector. By increasing the slope or decreasing the offset, the afternoon plasma drift would be downward instead of weakly upward as shown in Figure 9. This would correspond better with the CEJ shown in Figure 6, which implies a westward electric field at ~110 km altitude. The potential contribution of the neutral atmosphere is discussed below.

4.3. Neutral Response and Its Possible Contribution to the Ionospheric Disturbance

[26] The EEJ and plasma drift at the dip equator are mainly driven by the zonal electric field produced by the E region dynamo, hence dominantly related to the dynamical effects caused by lower atmospheric forcing. On the other hand, plasma density and TEC involve more complicated processes. These include not only the electrodynamics, but also background conditions in the thermosphere, like the composition, density, and wind.

[27] During the 2009 SSW event, the most prominent feature revealed by CHAMP is the substantial decrease in the neutral density of ~25% at 325 km altitude at low latitudes in the afternoon local time sector. It is important to point out that although only the Asian sector is shown in Figure 8, the neutral density decrease is observed at all longitudes. A thorough discussion about the strong neutral density decrease during the 2009 SSW event is reported by *Liu et al.* [2011]. Since neutral density is closely controlled by the neutral temperature, the large neutral density decrease demonstrates significant cooling in the equatorial upper thermosphere. This cooling precedes the SSW peak and the plasma depletion. Possible local effects on the neutral density, such as may occur from local wind perturbations due to plasma density or drift changes, are regarded to be minor for the global change.

[28] The cause of this thermosphere cooling is an interesting question. Considering the extremely low geomagnetic activity level ($K_p < 2$) during 19–25 January, geomagnetic activity effect can almost be confidently excluded. Also, the partial solar eclipse on 26 January 2009, which passed the Asian sector at local time after 18:00 LT, is impossible to cause the depression several days before the eclipse. Thus, this thermospheric density decrease may be potentially related to the occurrence of the SSW event.

[29] Cooling in the tropical stratosphere during SSW events is well known and was already observed several decades ago. It is explained as a result of upward air motion in the tropics related to the meridional circulation during SSWs [Julian and Labitzke, 1965; Fritz and Soules, 1970, 1972]. SSW-related cooling in the ionospheric F region at middle latitudes has also been detected by Goncharenko and Zhang [2008], using daytime ion temperature observed by the Millstone Hill radar. Since ion temperature at these heights is very close to the neutral temperature during day, their observations imply a cooling in the upper thermosphere at middle latitudes. Although it is not clear at this moment how these cooling are linked to the cooling in the equatorial upper thermosphere revealed in our study, and how chemical processes induced by the background thermosphere balance the dynamical processes driven by the equatorial fountain, our results open a new perspective for investigating thermosphere-ionosphere response to SSWs and points to a clear need for modeling the neutral and plasma processes simultaneously in the upper atmosphere.

5. Conclusions

[30] To conclude, our analysis of the ground and satellite observations in the Asian sector during the 2009 SSW event has revealed the following main features.

[31] First, TEC disturbances during the SSW are strongly latitudinal dependent, with monotonic depletion at the dip equator, but semidiurnal perturbation at low latitudes. This contrasts to an overall semidiurnal pattern in the Peruvian sector.

[32] Second, the TEC semidiurnal perturbation possesses a significant hemispheric asymmetry, being twice as strong in the Northern Hemisphere as that in the Southern Hemisphere. This contrasts to a stronger southern perturbation in the Peruvian sector.

[33] Third, the EEJ also experiences a semidiurnal perturbation, with strong counter electrojet occurring in the afternoon, similar to those observed in other longitude sectors during SSW events.

[34] Finally, the thermospheric density at low latitudes experiences ~25% decrease in the afternoon local time sector, indicating significant cooling in the equatorial upper thermosphere.

[35] **Acknowledgments.** We thank T. Tsuda for interesting discussions on the upward propagation of gravity waves and planetary waves. The magnetometer station at Kototabang is managed by the Solar-Terrestrial Environment Laboratory, Nagoya University, Japan. SEALION is managed by NICT, Japan, in collaboration with KMITL and CMU (Thailand), LAPAN (Indonesia), HIG/VAST (Vietnam), CSSAR/CAS (China), USC (Philippines), and Kyoto University (Japan). The work of H.L. and S.T.R. is supported by the JSPS grant.

[36] Robert Lysak thanks the reviewers for their assistance in evaluating this paper.

References

Abdu, M., T. K. Ramkumar, I. S. Batista, C. G. Brum, H. Takahashi, B. W. Reinisch, and I. H. Sobra (2006), Planetary wave signatures in the equatorial atmosphere-ionosphere system and mesosphere, E- and F-region coupling, *J. Atmos. Sol. Terr. Phys.*, *68*, 509–522.

Chau, J. L., B. G. Fejer, and L. P. Goncharenko (2009), Quiet variability of equatorial E × B drifts during a sudden stratospheric warming event, *Geophys. Res. Lett.*, *36*, L05101, doi:10.1029/2008GL036785.

Chau, J. L., N. A. Aponte, E. Cabassa, M. P. Sulzer, L. P. Goncharenko, and S. A. González (2010), Quiet time ionospheric variability over Arecibo during sudden stratospheric warming events, *J. Geophys. Res.*, *115*, A00G06, doi:10.1029/2010JA015378.

Fejer, B. G., M. E. Olson, J. L. Chau, C. Stolle, H. Lühr, L. P. Goncharenko, K. Yumoto, and T. Nagatsuma (2010), Lunar-dependent equatorial ionospheric electrodynamic effects during sudden stratospheric warmings, *J. Geophys. Res.*, *115*, A00G03, doi:10.1029/2010JA015273.

Forbes, J. M., and S. Leveroni (1992), Quasi 16-day oscillation in the ionosphere, *Geophys. Res. Lett.*, *19*, 981–984.

Fritz, S., and S. D. Soules (1970), Large-scale temperature changes in the stratosphere observed from Nimbus III, *J. Atmos. Sci.*, *27*, 1091–1097.

Fritz, S., and S. D. Soules (1972), Planetary variations of stratospheric temperature, *Mon. Weather Rev.*, *100*, 582–589.

Funke, B., M. López-Puertas, D. Bermejo-Pantaleón, M. García-Comas, G. P. Stiller, T. von Clarmann, M. Kiefer, and A. Linden (2010), Evidence for dynamical coupling from the lower atmosphere to the thermosphere during a major stratospheric warming, *Geophys. Res. Lett.*, *37*, L13803, doi:10.1029/2010GL043619.

Goncharenko, L., and S. Zhang (2008), Ionospheric signatures of sudden stratospheric warming: Ion temperature at middle latitude, *Geophys. Res. Lett.*, *35*, L21103, doi:10.1029/2008GL035684.

Goncharenko, L. P., J. L. Chau, H. Liu, and A. J. Coster (2010a), Unexpected connections between the stratosphere and ionosphere, *Geophys. Res. Lett.*, *37*, L10101, doi:10.1029/2010GL043125.

Goncharenko, L. P., A. J. Coster, J. L. Chau, and C. E. Valladares (2010b), Impact of sudden stratospheric warmings on equatorial ionization anomaly, *J. Geophys. Res.*, *115*, A00G07, doi:10.1029/2010JA015400.

Immel, T. J., E. Sagawa, S. L. England, S. B. Henderson, M. E. Hagan, S. B. Mende, H. U. Frey, C. M. Swenson, and L. J. Paxton (2006), Control of equatorial ionospheric morphology by atmospheric tides, *Geophys. Res. Lett.*, *33*, L15108, doi:10.1029/2006GL026161.

Julian, P. R., and K. B. Labitzke (1965), A study of atmospheric energetics during the January–February 1963 stratospheric warming, *J. Atmos. Sci.*, *27*, 597–610.

Kurihara, J., Y. Ogawa, S. Oyama, S. Nozawa, M. Tsutsumi, C. M. Hall, Y. Tomikawa, and R. Fujii (2010), Links between a stratospheric sudden warming and thermal structures and dynamics in the high-latitude mesosphere, lower thermosphere, and ionosphere, *Geophys. Res. Lett.*, *37*, L13806, doi:10.1029/2010GL043643.

Lastovicka, J. (2006), Forcing of the ionosphere by waves from below, *J. Atmos. Sol. Terr. Phys.*, *68*, 479–497.

Liu, H., and R. G. Roble (2002), A study of a self-generated stratospheric sudden warming and its mesospheric-lower thermospheric impacts using the coupled TIME-GCM/CCM3, *J. Geophys. Res.*, *107*(D23), 4695, doi:10.1029/2001JD001533.

Liu, H., H. Lühr, V. Henize, and W. Köhler (2005), Global distribution of the thermospheric total mass density derived from CHAMP, *J. Geophys. Res.*, *110*, A04301, doi:10.1029/2004JA010741.

Liu, H., H. Lühr, S. Watanabe, W. Köhler, V. Henize, and P. Visser (2006), Zonal winds in the equatorial upper thermosphere: Decomposing the solar flux, geomagnetic activity, and seasonal dependencies, *J. Geophys. Res.*, *111*, A07307, doi:10.1029/2005JA011415.

Liu, H., H. Lühr, S. Watanabe, and W. Köhler (2007a), Contrasting behavior of the equatorial ionosphere and thermosphere in response to the Oct. 28, 2003 solar flare, *J. Geophys. Res.*, *112*, A07305, doi:10.1029/2007JA012313.

Liu, H., C. Stolle, M. Förster, and S. Watanabe (2007b), Solar activity dependence of the electron density at 400 km at equatorial and low latitudes observed by CHAMP, *J. Geophys. Res.*, *112*, A11311, doi:10.1029/2007JA012616.

Liu, H., M. Yamamoto, and H. Lühr (2009), Wave-4 pattern of the equatorial mass density anomaly: A thermospheric signature of tropical deep convection, *Geophys. Res. Lett.*, *36*, L18104, doi:10.1029/2009GL039865.

Liu, H., W. Wang, A. D. Richmond, and R. G. Roble (2010), Ionospheric variability due to planetary waves and tides for solar minimum conditions, *J. Geophys. Res.*, *115*, A00G01, doi:10.1029/2009JA015188.

Liu, H., E. Doornbos, M. Yamamoto, and S. Tulasi Ram (2011), Strong thermospheric cooling during the 2009 major stratosphere warming, *Geophys. Res. Lett.*, *38*, L12102, doi:10.1029/2011GL047898.

Maruyama, T., M. Kawamura, S. Saito, K. Nozaki, H. Kato, N. Hemmakorn, T. Boonchuk, T. Komolmis, and C. H. Duyen (2007), Low latitude ionosphere-thermosphere dynamics studies with ionosonde chain in Southeast Asia, *Ann. Geophys.*, *25*, 1569–1577, doi:www.ann-geophys.net/25/1569/2007/.

Matsuno, T. (1971), A dynamical model of the stratospheric sudden warming, *J. Atmos. Sci.*, *28*, 1479–1494.

- McNamara, L., D. L. Cooke, C. E. Valladares, and B. W. Reinisch (2007), Comparison of CHAMP and Digisonde plasma frequencies at Jicamarca, Peru, *Radio Sci.*, *42*, RS2005, doi:10.1029/2006RS003491.
- Otsuka, Y., T. Ogawa, A. Saito, T. Tsugawa, S. Fukao, and S. Miyazaki (2002), A new technique for mapping of total electron content using GPS network in Japan, *Earth Planets Space*, *54*, 63–70.
- Pancheva, D. V., et al. (2006), Two-day wave coupling of the low-latitude atmosphere-ionosphere system, *J. Geophys. Res.*, *111*, A07313, doi:10.1029/2005JA011562.
- Pedatella, N. M., and J. M. Forbes (2010), Global structure of the lunar tide in the ionospheric total electron content, *Geophys. Res. Lett.*, *37*, L06103, doi:10.1029/2010GL042781.
- Prölss, G. (1980), Magnetic storm associated perturbations of the upper atmosphere: Recent results obtained by satellite-borne gas analyzers, *Rev. Geophys.*, *18*, 183–202.
- Prölss, G. (1993), Common origin of positive ionospheric storms at middle latitudes and the geomagnetic activity effect at low latitudes, *J. Geophys. Res.*, *98*, 5981–5991.
- Rusch, C. M., and A. D. Richmond (1973), The relationship between the structure of the equatorial anomaly and the strength of the equatorial electrojet, *J. Atmos. Terr. Phys.*, *35*, 1171–1180.
- Sagawa, E., T. J. Immel, H. U. Frey, and S. B. Mende (2005), Longitudinal structure of the equatorial anomaly in the nighttime ionosphere observed by IMAGE/FUV, *J. Geophys. Res.*, *110*, A11302, doi:10.1029/2004JA010848.
- Scherhag, R. (1952), Die explosionsartigen Stratosphärenenerwärmungen des Spätwinters 1951/1952, in *Berichte des Deutschen Wetterdienstes in der US-Zone 6*, vol. 38, pp. 51–63, Springer, Berlin.
- Sridharan, S., S. Sathishkumar, and S. Gurubaran (2009), Variabilities of mesospheric tides and equatorial electrojet strength during major stratospheric warming events, *Ann. Geophys.*, *27*, 4125–4130, doi:10.5194/angeo-27-4125-2009.
- Stolle, C., C. Manoj, H. Lühr, S. Maus, and P. Alken (2008), Estimating the daytime equatorial ionization anomaly strength from electric field proxies, *J. Geophys. Res.*, *113*, A09310, doi:10.1029/2007JA012781.
- Tulasi Ram, S., S. Su, and C. H. Liu (2009), FORMOSAT-3/COSMIC observations of seasonal and longitudinal variations of equatorial ionization anomaly and its interhemispheric asymmetry during the solar minimum period, *J. Geophys. Res.*, *114*, A06311, doi:10.1029/2008JA013880.
- Vineeth, C., T. K. Pant, and R. Sridharan (2009), Equatorial counter electrojets and polar stratospheric sudden warmings: A classical example of high latitude-low latitude coupling?, *Ann. Geophys.*, *27*, 3147–3153, doi:10.5194/angeo-27-3147-2009.
- Wan, W., L. Liu, X. Pi, M.-L. Zhang, B. Ning, J. Xiong, and F. Ding (2008), Wavenumber-4 patterns of the total electron content over the low latitude ionosphere, *Geophys. Res. Lett.*, *35*, L12104, doi:10.1029/2008GL033755.

E. Doornbos, Aerospace Engineering, Delft University of Technology, Kluyverweg 1, NL-2629 HS Delft, Netherlands.

H. Liu and K. Yumoto, Space Environment Research Center, Kyushu University, Fukuoka 812-8581, Japan. (huixin@serc.kyushu-u.ac.jp)

T. Nagatsuma and T. Tsugawa, National Institute of Information and Communications Technology, 4-2-1 Nukui-kita, Koganei 184-8795, Japan.

Y. Otsuka, Solar-Terrestrial Environment Laboratory, Nagoya University, Nagoya 464-8601, Japan.

C. Stolle, National Space Institute, DTU Space, Technical University of Denmark, Juliane Maries Vej 30, DK-2100 Copenhagen, Denmark.

S. Tulasi Ram and M. Yamamoto, Research Institute for Sustainable Humanosphere, Kyoto University, Kyoto 611-0011, Japan.